




Experimental measurement of the electrical of the electrical conductivity of single crystal olivine at high temperature and high pressure under different oxygen fugacities

Lidong Dai , Heping Li , Congqiang Liu , Tongdi Cui , Shuangming Shan , Changjun Yang , Qingyou Liu & Heming Deng

To cite this article: Lidong Dai , Heping Li , Congqiang Liu , Tongdi Cui , Shuangming Shan , Changjun Yang , Qingyou Liu & Heming Deng (2006) Experimental measurement of the electrical of the electrical conductivity of single crystal olivine at high temperature and high pressure under different oxygen fugacities, Progress in Natural Science, 16:4, 387-393

To link to this article: <http://dx.doi.org/10.1080/10020070612330009>

 Published online: 28 Sep 2006.

 Submit your article to this journal [↗](#)

 Article views: 1

 View related articles [↗](#)

 Citing articles: 5 View citing articles [↗](#)

Experimental measurement of the electrical conductivity of single crystal olivine at high temperature and high pressure under different oxygen fugacities*

DAI Lidong^{1,2}, LI Heping^{1**}, LIU Congqiang³, CUI Tongdi⁴, SHAN Shuangming¹,
YANG Changjun¹, LIU Qingyou¹ and DENG Heming¹

(1. Laboratory of the Earth's Interior Materials and Fluid Geochemistry, Institute of Geochemistry, Chinese Academy of Sciences, Guiyang 550002, China; 2. Graduate School of the Chinese Academy of Sciences, Beijing 100039, China; 3. Institute of Geochemistry, Chinese Academy of Sciences, Guiyang 550002, China; 4. Guizhou University, Guiyang 550004, China)

Received July 25, 2005

Abstract At 1.0—4.0 GPa and 1123—1473 K and under oxygen fugacity-controlled conditions (Ni + NiO, Fe + Fe₃O₄, Fe + FeO and Mo + MoO₂ buffers), a YJ-3000t Model six-anvil solid high-pressure apparatus and a Sartlron-1260 Impedance/Gain-Phase analyzer were employed to conduct an *in situ* measurement of the electrical conductivity of single crystal olivine. Experimental results showed that: (1) within the range of experimentally selected frequencies (10³—10⁶ Hz), the electrical conductivity of the sample is of great dependence on the frequency; (2) with the rise of temperature (T), the electrical conductivity (σ) will increase, and the Arrhenius linear relationship is established between $\lg\sigma$ and $1/T$; (3) under the control of oxygen buffer Fe + Fe₃O₄, with the rise of pressure, the electrical conductivity tends to decrease whereas the activation enthalpy and independent-of-temperature preexponential factor tend to increase, with the activation energy and activation volume of the sample estimated at (1.25 ± 0.08) eV and (0.105 ± 0.025) cm³/mol, respectively; (4) under given pressure and temperature conditions, the electrical conductivity tends to increase whereas the activation energy tends to decrease with increasing oxygen fugacity; and (5) the mechanism of electrical conduction of small polarons can provide insight into the behavior of electrical conduction of olivine under high pressure and high temperature.

Keywords: olivine, high temperature and high pressure, electrical conductivity, oxygen fugacity, small polaron.

It is well known that olivine is one of the most important components in the upper mantle and it is also a predominant conductor in the mantle minerals. Therefore, geo-physicists engaged in research on the physical properties of solid Earth's interior materials have put their focus on olivine for a long time. The properties of isomorphs of its single crystal and polycrystal as well as synthetic olivine and α -olivine (Wadsleyite, namely β -olivine is present at the depth of 410—550 km in the mantle transitional zone, Ringwoodite, namely γ -olivine exists at the depth of 550—670 km in the mantle transitional zone) have been investigated systematically^[1–3].

In various high-temperature and high-pressure experiments, if the samples contain valence-varying elements, oxygen fugacity, like temperature and pressure, would become one of the most important external factors affecting experimental results. And the *in situ* control of oxygen fugacity in the dry sample system at high pressure has long been a puzzle for

the international high-pressure academic circles^[4]. Because exceedingly sophisticated facilities and experimental technologies are required, previous data were obtained under such conditions that the *in situ* control of oxygen fugacity at high pressure was not taken into consideration or the experiment was conducted below the pressure of 0.1 MPa. Therefore, the data obtained under high pressure and oxygen fugacity-controlled conditions are extremely limited^[5–7]. In regard to the controlling methodology, the high-pressure data so far reported were obtained basically by using one single buffer to control the oxygen fugacity of the sample^[8], and no similar report is available on the simultaneous use of different buffers to control the oxygen fugacity of the same mineral. Although Xu et al.^[9] have successively applied impedance spectroscopy to the *in situ* measurement of electrical conductivity of perovskite at high temperature and high pressure, and their method has been accepted internationally as the most advanced method of *in situ* experimental measurement of the electric properties of

* Supported by CAS Knowledge-Innovation Key Orientation Project (Grant No. KZCX3-SW-124), CAS One-Hundred Talented Personnel Program, and the National Natural Science Foundation of China (Grant No. 49674221)

** To whom correspondence should be addressed. E-mail: Hepingli@public.gz.cn

solid Earth's interior materials at high temperature and high pressure. However, till now, no relevant report is available on the systematic study of electrical conductivity of olivine—one extremely important single crystal mineral in the upper mantle at high pressure under the control of different oxygen buffers. In this work, we tried to perform an *in situ* measurement of the electrical conductivity of olivine at 1.0—4.0 GPa and 1123—1473 K under the control of four different oxygen buffers (Ni + NiO (NNO), Fe + Fe₃O₄ (IM), Fe + FeO (IW), and Mo + MoO₂ (MMO)) with the employment of impedance spectroscopy in the frequency range of 10³—10⁶ Hz, explore the impact of frequency, temperature and pressure on the measurements of electric properties at high temperature and high pressure, and calculate some important physical parameters such as preexponential factor, activation enthalpy, activation energy and activation volume, which determine the electric properties of minerals at high pressure.

Table 1. The chemical composition of olivine sample (wt %)

Composition	Cr ₂ O ₃	NiO	MnO	FeO	Na ₂ O	K ₂ O	Al ₂ O ₃	CaO	MgO	TiO ₂	SiO ₂
Content	0.39	0.41	0.61	12.41	0.01	0.15	0.12	0.16	45.64	0.02	41.94

The buffers were composed of fully mixed 99.99% purity metals and corresponding metal oxides: 79wt% Ni + 21wt% NiO, 72wt% Fe + 28wt% Fe₃O₄, 78wt% Fe + 22wt% FeO, and 75wt% Mo + 25wt% MoO₂, which were fully mixed respectively. The powder was crushed and sintered (sintering during: 2.5 h) at the Chinese General Academy of Iron and Steel with the help of the hot equal static pressing technique (133 MPa, 1573 K and argon gas protection), then the sintered massive specimens were proceeded into disk-like buffer electrodes (Φ5.0 mm × 1.0 mm) at Factory 185 under the Aviation-Space Ministry of China with the help of electrical spark discharge to erode the sintered specimens.

2 Experimental methods

The experiment was conducted on a YJ-3000t Model solid six-anvil high-pressure apparatus. For the details of the apparatus, please see Ref. [10].

In the experiment the pressure increased at a rate of 1.5 GPa/h to the assigned value. Under a constant pressure condition the temperature was raised slowly at a rate of 160 K/h to the preset value and the temperature interval between the adjacent preset values

1 Preparation of samples and buffers

Olivine samples used in the experiment were collected from nodular inclusions occurring in alkali-rich basalts at Xiaomaping area, Hebei Province, China. Olivine specimens were selected carefully from a large number of gem-grade samples, which are free from fissures and have inclusions growing along the crystal axis [001]. Electron microprobe and transmission electron microscope observations showed that the samples contain no serpentine and chlorite and their chemical compositions are listed in Table 1. Prior to experiment, olivine sample was first cut into cylinders with 5.92 mm in diameter and 5.95 mm in length, then immersed in acetone, washed with ultrasonic waves to eliminate oil dirt on the surface of the sample, and finally the prepared sample cylinders were placed in a 393 K baking oven for 24 h so as to remove adsorbed water on the surface of the sample completely.

was 50 K. After the temperature was raised to each preset value under constant pressure condition, the system was kept constant for a sufficiently long period of time (2—3 h) to reach buffering equilibrium. Then, with the ZPlot program on a Sarltron-1260 Impedance/Gain-Phase analyzer (measuring precision: 0.05%), the modulus $|Z|$ and phase angle Φ of complex impedance for the sample were worked out within the frequency range of f (10³—10⁶ Hz). According to the following formulae:

$$Z_r = |Z| \cos\theta, \quad (1)$$

$$Z_i = |Z| \sin\theta, \quad (2)$$

we calculated the real part Z_r and imaginary part Z_i of complex impedance, then fitted the results of Z_r and Z_i by operating the ZView program in accordance with an equivalent electric circuit, and finally we obtained the resistance value of the sample at given temperature, pressure and oxygen fugacity. According to Refs. [1, 6, 9], the fitting electric circuit is made up of an ohmic electrical resistor representing the intrinsic conduction mechanism of a sample and an electric capacitor which is made up of two parallel electrodes, with the ohmic resistance connected in parallel with the electric capacitor.

The experimental sample set-up is shown in Fig. 1. The whole sample block size was 32.5 mm ×

32.5 mm × 32.5 mm. To avoid the influence of dehydration on the measurement of electrical conductivity, pyrophyllite was baked to 973 K prior to sample assemblage to let the mineral dehydrate completely. To control the partial pressure of oxygen in the sample chamber and reduce the influence of surface electric current in the process of conductivity measurement, the electrodes were made from solid oxygen buffers (as large as $\Phi 5$ mm × 1.0 mm). The heater was composed of three layers of stainless steel sheet. The temperature was measured with a Pt/PtRh₁₀ thermocouple, because the total error of temperature caused by the temperature gradient in the sample chamber did not exceed 10 K. In addition, a shield cover made of metallic foil was installed in the sample set-up, and the composition of metallic foil was similar to that in the buffers. Compared with the routinely used shield tubes^[19], our shield cover, owing to its consecutive sealing, has the advantages of more effectively shielding the external electromagnetic interference, blocking up the stray current, reducing the temperature gradient in the sample chamber and controlling the partial pressure of oxygen in the sample chamber.

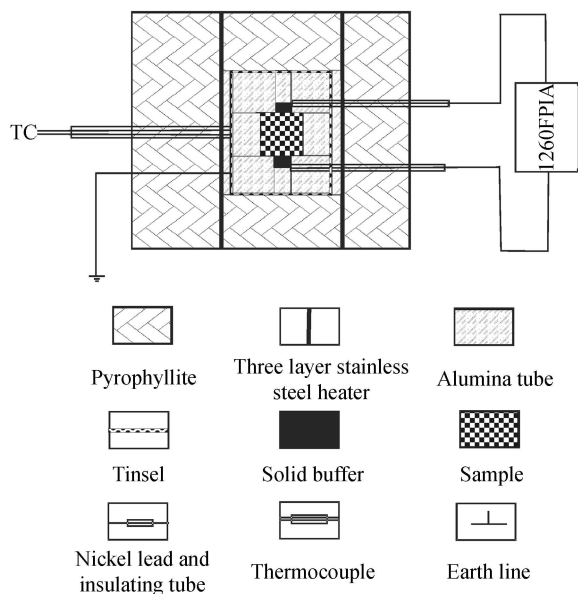


Fig. 1. Schematic diagram of the experimental set-up.

3 Results and discussion

In this work the impedance spectroscopic measurements of olivine were obtained respectively at 1.0—4.0 GPa and 1123—1473 K under Fe + Fe₃O₄ buffer and at 2.0 GPa and 1123—1473 K under NNO, IM, IW and MMO buffers. The frequency span of impedance spectra is 10³—10⁶ Hz.

Shown in Fig. 2 are the results of impedance spectroscopic measurements for samples at 2.0 GPa and 1123—1473 K with Fe + Fe₃O₄ as the buffer. The results obtained under other conditions are similar to those shown in Fig. 2. It can be seen that the circular arc representing the grain interior conduction mechanism of the sample and appearing over a high frequency range tends to become more and more perfect with the rise of temperature and its diameter tends to become smaller and smaller. The circular arc passes through the origin, and its center and diameter both fall on the real axis. According to the principle of impedance spectroscopy^[6], it is known that the diameter of the circular arc represents the intrinsic resistance R of the sample. From this it can be seen clearly that the impedance of the grain interior is of great dependence on temperature. The semicircular arc representing the conduction mechanism between the sample and the electrodes appeared over the low frequency range (10⁻¹—10³ Hz), and due to the insufficient span of low frequency range, the impedance arc resultant from this conduction mechanism on the complex plane has not yet been identified in this work. From the Z' versus Z'' plot it can also be seen that the electrical conductivity of olivine is determined predominantly by the grain interior conduction mechanism, and the transmission between the sample and the electrodes does not reflect the intrinsic conduction of the sample. So it was not taken into consideration. From this it can be seen that the electrical conductivity of the sample is of great dependence on temperature.

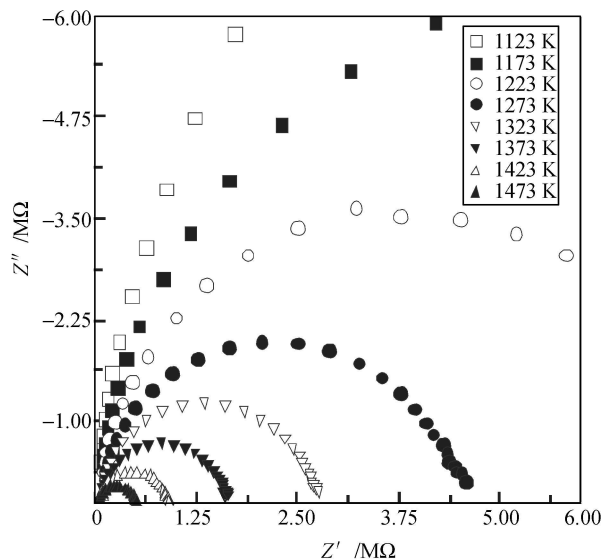


Fig. 2. Z' vs. Z'' plot of complex impedance of olivine at 1 kHz—1 MHz (from right to left), obtained under the conditions of 2.0 GPa, 1123—1473 K, and IM buffer. Z' and Z'' are the real and imaginary parts of complex impedance.

Fig. 3 shows the relationships between modulus and frequency and between phase angle and frequency at 2.0 GPa and 1124–1473 K. It can be seen that $|Z|$ and θ of the complex impedance vary continuously and regularly with f , and $|Z|$ is of great dependence on f . Over the high frequency range (10^3 – 10^6 Hz), $|Z|$ tends to increase rapidly with f , varying from high to low value, but the variation gradient will become smaller and smaller. When f reaches 10^3 Hz, $|Z|$ will generally maintain a constant value. The phase angle, θ , of complex impedance is also of great dependence on frequency f . In the frequency of 10^6 Hz recorded at 2.0 GPa and 1123 K, the absolute value of θ is 53° ; when scanning from 10^6 Hz to 2×10^5 Hz, $|\theta|$ will reach its maximum value, 78° . After one time of turning, $|\theta|$ will begin to become small slowly and finally approach zero. The relationship between $|Z|$ and θ of complex impedance and Z_r and Z_i just satisfies Eqs. (1) and (2). From this it can be deduced that the modulus, $|Z|$, and phase angle, θ , of olivine are greatly dependent on frequency, f , and σ of the sample also greatly depends on f .

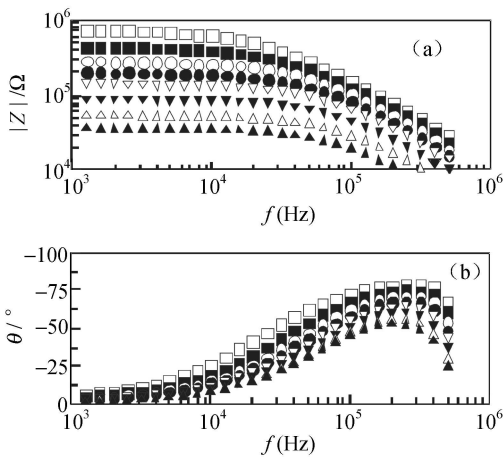


Fig. 3. Dependence of the modulus, $|Z|$, and phase angle, θ , of complex impedance of olivine on frequency, f , under the conditions of 2.0 GPa and 1123–1473 K. For symbols refer to Fig. 2.

All the impedance spectra obtained in the experiment are fitted with the ZView program to work out the impedance of the sample. The impedance is substituted into Eq. (3) to calculate the electrical conductivity:

$$\sigma = \frac{L/S}{R} = \frac{L}{SR}, \quad (3)$$

where σ is the electrical conductivity (S/m), L the length of the sample (m), S the cross section (m^2),

and R the impedance (Ω) of the sample. From Eq. (3), we can calculate the electrical conductivities under different temperature, pressure and oxygen fugacity conditions. Fig. 4 is the plot of $\lg \sigma$ versus $1/T$. Under the 1.0–4.0 GPa conditions there is a good linear correlation between $\lg \sigma$ and $1/T$, and the squares of correlation coefficients between ΔH and σ_0 are 0.9988, 0.9975, 0.9929 and 0.9954, respectively. Such a good correlation is related directly to the 50 K temperature interval only. The plots of $\lg \sigma$ versus ($1/T$) under the four pressure conditions all satisfy the Arrhenius's formula:

$$\sigma = \sigma_0 \exp(-\Delta H/kT), \quad (4)$$

$$\Delta H = \Delta U + P \times \Delta V, \quad (5)$$

where σ is the electrical conductivity (S/m), σ_0 the preexponential factor independent of temperature (S/m), k the Boltzmann constant, T the absolute temperature (Kelvin), ΔH the activation enthalpy (eV), ΔU the activation energy (eV), P the pressure (GPa), and ΔV the activation volume (cm^3/mol).

Table 2 gives the fitted parameters of Arrhenius relation for the sample. It can be seen that: (i) under the control of oxygen buffer IM, with the rise of pressure (P), ΔH and σ_0 will increase simultaneously. From 1.0 GPa to 4.0 GPa, ΔH tends to increase to 0.20 eV and σ_0 shows a slight increase, varying on the order of 10^2 – 10^3 S/m, relatively stable; (ii) by substituting the value of ΔH obtained at 1.0–4.0 GPa and under the control of oxygen buffer IM into Eq. (5), the ΔU and ΔV of the sample were worked out to be (1.25 ± 0.08) eV and (0.105 ± 0.025) cm^3/mol , respectively. The ΔU obtained in this work and ΔU (1.17–1.50 eV) obtained by Xu et al.^[11] from San Carlos olivine developed along different crystal axes at 4–10 GPa and 1273–1673 K under the control of buffers Mo + MoO₂ both fall within the same range of variations, though there exists a significant difference between ΔH and ΔU . It may be a reasonable explanation that there is a direct relation between the iron content of the sample and the controlled partial pressure of oxygen. The fact that ΔV is a very small decimal fraction indicates that the sample experienced slight lattice deformation with the rise of pressure; (iii) under the pressure of 2.0 GPa, ΔH tends to increase in succession in the order of NNO, IM, IW and MMO, and σ_0 shows no dependence on any oxygen buffer.

Table 2. Fitted parameters of Arrhenius relationship for the electrical conductivity of olivine

Oxygen buffer	P (GPa)	$\lg\sigma_0$	ΔH (eV)	σ ($S \cdot m^{-1}$)
IM	1.0	1.96	1.34	91.20
IM	2.0	2.19	1.43	154.88
IM	3.0	2.54	1.56	346.74
IM	4.0	2.74	1.64	549.54
NNO	2.0	2.05	1.35	112.20
IW	2.0	2.18	1.48	151.36
MMO	2.0	2.34	1.59	218.78

Fig. 4 shows the $\lg\sigma$ versus $1/T$ plot, which reflects the influence of pressure on electrical conductivity. The temperatures and four pressures selected in this experiment approximate to the upper-mantle conditions. It can be seen clearly that under the same temperature, the rise of pressure will lead to the drop of electrical conductivity. The relationship between the electrical conductivity of olivine and pressure has been well documented by previous scientists. In the study of the electrical conductivity of sintered polycrystalline olivine— $(Mg_{1-x}Fe_x)_2SiO_4$ at 2.9—7.0 GPa, 900—1900 K and 0.32 kHz under the uncontrolled partial pressure of oxygen, Omura et al.^[5] found that the electrical conductivity of Fe-low ($0 < x < 50\%$) olivine decreased with increasing pressure, whereas the electrical conductivity of Fe-high olivine ($50\% < x < 1$) increased with increasing pressure. Xu et al.^[11] has made the same conclusion in their study of the influence of pressure on the electrical conductivity of San Carlos olivine over the frequency range of 1 kHz—1 MHz, i.e. the electrical conductivity of Fe-low olivine tends to decrease with increasing pressure. This provides great support to the viewpoint of Omura et al.^[5]. Differences in iron contents led to an extremely reversed rule of variation of electrical conductivity with pressure, which can be reasonably explained by the differences in conduction mechanism. The main conduction mechanism of Fe-low olivine is the small polaron conduction, while that of Fe-high olivine is the ion conduction^[12]. The calculated Fe/(Mg + Fe) ratio of 13.1% from Table 1 is close to that (10%) of San Carlos olivine selected by Xu et al.^[11], satisfying the rule of variation of the electrical conductivity of Fe-low olivine with pressure with small polarons playing the leading role in electrical conduction. Meanwhile, Xu et al.^[11] also thought that the value of activation volume for the ion conduction mechanism is higher than $1.0 \text{ cm}^3/\text{mol}$, but the activation volume that varies on the order of $0.5 \text{ cm}^3/\text{mol}$ usually refers to small polaron conduction. How-

ever, in any case, it is the first trial to systematically study, using the impedance spectroscopy across the order of magnitude of 10^3 and by selecting such a low frequency, the relationship between the electrical conductivity of Fe-low olivine and pressure at 1.0—4.0 GPa and 1123—1473 K and under the control of buffer IM.

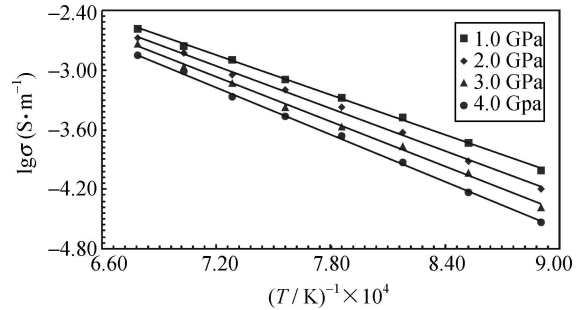


Fig. 4. $\lg \sigma$ versus $1/T$ for olivine under the conditions of 1.0—4.0 GPa and buffer IM.

Previous studies showed that there exist significant differences in oxygen fugacity in different spaces and tectonic settings of the upper mantle, but the values vary from IW (Fe + FeO) to FQM (fayalite + SiO_2 + magnetite)^[4]. In accordance with the descending order of oxygen fugacity, four solid oxygen buffers NNO, IM, IW and MMO were selected in this work to control the oxygen fugacities in the sample chamber, and their theoretically calculated data are given in Table 3. From the table we can see that oxygen fugacity is the odd-value function of temperature and pressure, and under the control of the same buffer the oxygen fugacity tends to increase with the rise of temperature and the drop of pressure. Under the same temperature and pressure conditions, different oxygen buffers show obviously different buffering capacities. In the order of NNO, IM, IW and MMO, the buffering capacity, the oxidation ability

Table 3. Theoretically calculated data of $\log f_{O_2}$ (f_{O_2} : bar) at high temperature and high pressure*

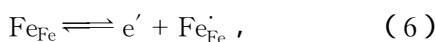
Oxygen buffer	A	B	C	According to Ref.
NNO	-24930	9.36	0.046	[15]
IM	-29260	8.99	0.061	[13]
IW	-27215	6.57	0.052	[14]
MMO	-30650	8.92	0.054	[11]

* $\log(f_{O_2})_{P,T} = A/T + B + C(P-1)/T$, where T is the absolute temperature (Kelvin); P is the pressure (bar); $C = -\Delta V_S / 2.303R$, ΔV_S stands for the bulk variation in mol volume of solid components before and after buffering reaction (cm^3/mol); R is the gas state constant ($\text{cm}^3 \cdot \text{atm}/\text{mol} \cdot \text{K}^{-1}$).

Downloaded by [University of California, San Diego] at 13:16 29 June 2016

and oxygen fugacity tend to be weaker, and the reduction ability tends to be stronger^[11,13-15]. From them IM was selected because it mostly approximates to the oxygen fugacity (FQM) on the margin at the top of the upper mantle. Experiments were conducted under different pressures and IM buffer, and comparisons were made at 2.0 GPa under the control of different oxygen buffers.

Fig. 5 is the plot of $\lg \sigma$ versus $1/T$ established at 2.0 GPa and 1123—1473 K under the control of four different buffers NNO, IM, IW and MMO. It can be seen that under the conditions of different temperatures and pressures, the electrical conductivity (σ) of a single crystal of olivine and oxygen fugacity (f_{O_2}) show a variation trend in the same direction, i.e. σ increases with the increasing f_{O_2} and *vice versa*. Evidence is available for the increase of positive thermoelectrical coefficient data^[16], dielectric constant^[17] and electrical conductivity with increasing iron content below 1663 K, and under 0.1 MPa there exists a positive correlation between σ and f_{O_2} ^[19]. It is indicated that Fe-low olivine is dominated by small polaron conduction, and small polaron conduction mechanism of the sample provided a reasonable explanation to the rule of variation of electrical conductivity with oxygen fugacity. Electron microprobe analysis indicated that the valence-varying element iron in single crystal olivine presented mainly in the form of Fe^{2+} . According to the principle of lattice point defects^[20], under a certain temperature condition atomic exchange would necessarily occur between oxygen gas sealed in the sample chamber and Fe^{2+} in the sample, leading to the occurrence of point defect reduction-oxidation reaction. As a result, iron (Fe_{Fe}) which occupied the lattice site of iron and Fe^{2+} in the structure of olivine was oxidized into small polarons (Fe_{Fe}^{\cdot}), and at the same time, vacancies and holes, which are the main forms of defects, were produced in the process of reaction. However, with the time passing by, Fe_{Fe} and Fe_{Fe}^{\cdot} reached the state of buffering equilibrium. Later, Fe_{Fe} and Fe_{Fe}^{\cdot} respectively maintained their own concentrations. Electrical conduction of small polarons in the sample was affected with the help of cavities at the lattice ferrous iron site and transition among small polarons. The process of transition is expressed as:



where Fe_{Fe} indicates the site the bivalent iron ion oc-

cupies, e' represents electron, and Fe_{Fe}^{\cdot} denotes small polaron. With the increasing of the temperature, vacancies and holes in the sample would separate with each other; the cavities would transit from Fe_{Fe} to Fe_{Fe}^{\cdot} . At the same time, a ferrous iron ion vacancy was produced. In a periodical manner, like Fe_{Fe}^{\cdot} , it is transferred in the lattice, marking a process of electrical conduction of single crystal olivine. Under the control of oxygen buffer IM, with the increasing of pressure, the concentrations of point defects produced along with point-defect oxidation-reduction reaction tend to increase, electrical conductivity is positively correlated with defect concentrations, electrical conduction intensifies and electrical conductivity increases. Under the control of oxygen buffer IM, with the increasing of pressure, the concentrations of free oxygen sealed in the sample chamber, produced by point defects, the distance of polar transition and the electrical conductivity tend to decrease, however activation enthalpy increases. At 2.0 GPa, the oxygen fugacity increased in the order of MMO, IW, IM and NNO, and the concentrations of small polarons produced by point-defect oxidation-reduction reaction increased, electrical ability intensified, electrical conductivity increased, and at the same time the distance of polar transition increased, however activation enthalpy decreased.

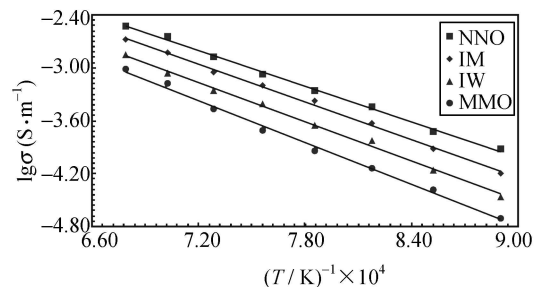


Fig. 5. $\lg \sigma$ versus $1/T$ for olivine under the conditions of 1.0—4.0 GPa and different buffers.

4 Conclusions

In the paper, by virtue of impedance spectroscopic methods we measure the electrical conductivity of olivine under conditions of 1.0—4.0 GPa, 1123—1473 K and controlling the oxygen partial pressure. The controlling oxygen fugacity consists of four buffers: NNO, IM, IW and MMO. It is the first time that the activation energy and activation volume of the sample have been estimated at (1.25 ± 0.08) eV and (0.105 ± 0.025) cm³/mol, respectively. The

electrical conductivity of the olivine is manifested to be dependent on T , P and f_{O_2} . With the temperature and the oxygen fugacity increasing, the electrical conductivity enhances. With the pressure increasing, the electrical conductivity decreases. The mechanism of electrical conduction of small polarons can provide reasonable explanations to the behavior of electrical conduction of olivine at high pressure and high temperature.

Acknowledgements Senior Engineer Zhao Shunxing of the General Academy of Iron and Steel of China accomplished part of work involved in hot equal crystal pressing. Factory 185 under the Aviation and Space Industry Ministry provided the electrical spark discharge-erosion technique and helped preparing the buffers. Senior Engineer Wang Mingzai of the Institute of Geochemistry, Chinese Academy of Sciences conducted electron microprobe analysis on samples. Here the authors would like to extend their special thanks to them all.

References

- 1 Xu Y. S., Poe B. T., Shankland T. J. et al. Electrical conductivity of olivine, wadsleyite, and ringwoodite under upper-mantle conditions. *Science*, 1998, 280 : 1415—1418.
- 2 Toru I., Tanimoto Y., Irifune T. et al. Thermal expansion of wadsleyite, ringwoodite, hydrous wadsleyite and hydrous ringwoodite. *Phys. Earth Planet Inter.*, 2004, 143 : 279—290.
- 3 Wenk H. R., Lonardelli I., Pehl J. et al. *In situ* observation of texture development in olivine, ringwoodite, magnesiowüstite and silicate perovskite at high pressure. *Earth and Planetary Science Letters*, 2004, 226 : 507—519.
- 4 Li H. P., Xie H. S., Guo J. et al. *In situ* control oxygen fugacity at high temperature and high pressure: A Ni-O system. *Geophysical Research Letters*, 1998, 25(6) : 817—820.
- 5 Omura K., Kurita K. and Kumazawa M. Experimental study of pressure dependence of electrical conductivity of olivine at high temperatures. *Phys. Earth Planet Inter.*, 1989, 57 : 291—303.
- 6 Huebner J. S. and Dillenaug G. D. Impedance spectra of dry silicate minerals and rock: qualitative interpretation of Spectra. *Am. Mineral.*, 1995, 80 : 46—64.
- 7 Lemelle L. P., Duba A. G. and Guyot F. The electrical conductivity of olivine under highly reducing conditions. *Phys. Chem. Minerals.*, 1998, 26 : 164—170.
- 8 Yasuda A. and Fujii T. Application of a solid-electrolyte oxygen fugacity sensor to high-pressure experiments. *Phys. Earth Planet Inter.*, 1993, 80 : 49—64.
- 9 Xu Y. S., McCammon C. and Poe B. T. The effect of alumina on the electrical conductivity of silicate perovskite. *Science*, 1998, 282 : 922—924.
- 10 Xie H. S., Zhou W. G., Zhu M. X. et al. Elastic and electrical properties of serpentine dehydration at high temperature and high pressure. *J. Phys B: Condensed Matter.*, 2002, 14(44) : 11359—11363.
- 11 Xu Y. S., Shankland T. J. and Duba A. G. Pressure effect on electrical conductivity of mantle olivine. *Phys. Earth Planet. Inter.*, 2000, 118 : 149—161.
- 12 Li L., Raterron O., Weidner D. et al. Olivine flow mechanisms at 8.0 GPa. *Phys. Earth Planet Inter.*, 2003, 138 : 113—129.
- 13 O'Neill S. C. Systems Fe-O and Cu-O: Thermodynamic data for the equilibria Fe-FeO, Fe-Fe₃O₄, FeO-Fe₃O₄, Fe₃O₄-Fe₂O₃, Cu-Cu₂O, and Cu₂O-CuO from emf measurements. *Am. Mineral.*, 1988, 73 : 470—486.
- 14 Hirsch L. M. The Fe-FeO buffer at lower mantle pressures and temperatures. *Geophysical Research Letters*, 1991, 18(7) : 1309—1312.
- 15 Li H. P., Xie H. S., Guo J. et al. *In situ* control oxygen fugacity at high temperature and high pressure. *J. Geophys. Res.*, 1999, 104(B12) : 29439—29451.
- 16 Shock R. N., Duba A. and Shankland T. J. Electrical conduction in olivine. *J. Geophys. Res.*, 1989, 94 : 5829—5839.
- 17 Wanamaker B. J. and Duba A. G. Electrical conductivity of San Carlos olivine along [100] under oxygen- and pyroxene-buffered conditions and implications for defect equilibria. *J. Geophys. Res.*, 1993, 98(B1) : 489—500.
- 18 Constable S. C., Shankland T. J. and Duba A. The electrical conductivity of an isotropic olivine mantle. *J. Geophys. Res.*, 1992, 97 : 3397—3402.
- 19 Duba A. and Constable S. C. The electrical conductivity of iherzolite. *J. Geophys. Res.*, 1993, 98(B7) : 11885—11899.
- 20 Wanamaker B. J. Point defect diffusivities in San Carlos olivine derived from reequilibration of electrical conductivity following changes in oxygen fugacity. *Geophysical Research Letters*, 1994, 21(1) : 21—24.